Frequency offset estimation in the intermediate frequency for satellite-based AIS signals*

MENG Xin (孟鑫)[1,2]**, **MA She-xiang** (马社祥)[3], **LIU Chen** (刘琛)[3], **and TENG Jian-fu** (滕建辅)[1]

1. School of Electronic Information Engineering, Tianjin University, Tianjin 300072, China

2. Maritime College, Tianjin University of Technology, Tianjin 300384, China

3. School of Electrical and Electronic Engineering, Tianjin University of Technology, Tianjin 300384, China

(Received 26 March 2018; Revised 1 May 2018)

In this paper, an accurate frequency offset estimator is investigated in the intermediate frequency for the satellite-based automatic identification system (AIS) signals. Using Gaussian minimum shift keying (GMSK) modulation for transmission, the AIS signal is shown to be a plane wave with the modulated phase information and carrier frequency resulting from the Doppler effects. Hence, the phase information can be eliminated with a re-modulated signal, and the frequency offset can be estimated by the ratio of the maximum spectral amplitude and its neighbor spectral amplitude based on the fast Fourier transformation (FFT) interpolation. The estimator has low complexity, and it is easy to implement. Computer simulations are used to assess the performance of the estimator.

Document code: A **Article ID:** 1673-1905(2018)04-0301-5

DOI https://doi.org/10.1007/s11801-018-8044-7

Automatic identification system (AIS) is defined to improve navigation safety and maritime surveillance, and it is applied to avoid the occurrence of collision and other accidents in its work cell. However, the radius of the AIS work cell is less than 40 nautical miles[1], which makes it difficult to meet the ship monitoring worldwide. Thus, the satellite-based AIS is a viable option[2]. In the satellite-based AIS, the low-earth-orbit (LEO) constellation of small size satellites is usually assumed for global coverage, with an altitude ranging from 600 km to 1 000 km. For typical LEO altitudes and field of view (FoV) in AIS applications, there are lots of problems[3,4], the receiver moves at the speed of 7 km/s relative to the ships, and the maximum Doppler shift is approximately ±3.8 kHz[5]. Additionally, the signal-to-noise ratio (*SNR*) is 0—20 dB due to the complex atmospheric environment and the distant transmission[6]. The correct frequency offset is perquisite for demodulating the received AIS signals.

The AIS signal is modulated by Gaussian minimum shift keying (GMSK), and the frequency offset estimation methods for GMSK are typically categorized in non-data-aided (NDA) ones and data-aided (DA) ones[6], and the former is focused in this paper. Based on the least square (LS) criterion, the classic Kay method which utilizes the phase differences between adjacent signals was proposed in Ref.[7], but it has poor performance at low *SNR*, and the estimation range is a quarter of the bit rate. A maximum likelihood (ML) frequency estimator was proposed in Ref.[8], and it removed the phase information with the help of available data, eventually the frequency was obtained from the autocorrelation function. Although its estimation accuracy is remarkably high, its operating range is limited to a few percent of the bit rate. Based on the Taylor series expansion, Ref.[9] shows an open-loop digital frequency offset estimation technique. Ref.[10] presents a modified method by means of the Laurent expansion, which is a shortcut of the method in Ref.[9]. The methods of Ref.[9] and Ref.[10] have low computational complexity and high estimation accuracy, but their estimation ranges are around ten percent of the bit rate. Ref.[11] investigates frequency recovery by means of fast Fourier transformation (FFT) and the recursion structure, and this method consists of a coarse frequency corresponding to the maximum amplitude FFT coefficient and a fine frequency resulting from the modified discrete Fourier transform (DFT) coefficients, which are defined by the maximum spectral number. The performance depends on the time of iteration and FFT length, and it has high computational complexity. Nevertheless, the estimator performs poorly at low *SNR* when the number of FFT points is not moderately long. Ref.[12] develops a two-ray spectrum approximate model for the Doppler spread estimation. Finally, the Doppler spread as well as the CFO is obtained, but the estimator performs poorly. Ref.[13] proposes a new frequency estimator for the satellite-based AIS signals, the Laurent approximation is used to remove the phase information, and then the frequency offset is estimated by means of

* This work has been supported by the National Natural Science Foundation of China (No. 61601326).

** E-mail: mengxin@tjut.edu.cn

autocorrelation and DFT. However, the estimator needs long data, which is unavailable in practice. Ref.[14] proposes a joint recovery scheme for carrier frequency offset and phase noise utilizing extended Kalman filter for QPSK signal.

Considering that the frequency diversity of the multi-user signals is a significant advantage for coarse separation, a satellite-based AIS receiver operating in the intermediate frequency can be conceived, and its block diagram is shown in Fig.1. In view of this situation, a frequency offset estimation method for the intermediate frequency is proposed in this paper. The phase modulation can be removed by the connatural symbol in the AIS frame, and the ratio of the maximum FFT spectral amplitude and its neighbor spectral amplitude can be utilized to acquire the frequency offset. This method is easy to implement and suitable for real time system. The simulation results show that the estimator has large estimation range and good performance, which is very close to the modify Cramer-Rao bound (MCRB).

Following the diagram of Fig.1, the received AIS signal from VHF antenna is multi-user mixed signal with frequency diversity due to the elevation and azimuth angle, whose power is amplified in the RF front-end, and the signal is down-converted to the intermediate frequency. Filtering the interference out of the band by the intermediate frequency filter, the signal is cursorily separated by the exploitation of the frequency diversity given by the Doppler shift in the zonal filter, and the intermediate frequency multi-user mixed signal is separated finely in the signal separation block. After that, the processed signal is used to estimate the time delay and frequency offset, which is compensated to the signal for demodulation.

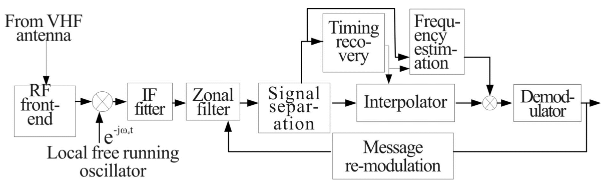

Fig.1 Block diagram of the satellite-based AIS receiver

The complex envelope of the transmitted AIS frame can be written as

$$s(t)=\mathrm{e}^{\mathrm{j}\phi(t;\alpha)}\ , \tag{1}$$

where

$$\phi(t;\alpha)=\pi h\sum_i \alpha_i q(t-iT_\mathrm{b}) \tag{2}$$

is the information bearing phase. In the above equation, $\alpha=\{\alpha_i\}$ are binary information sequences taking on the values ±1 with equal probability, and T_b is the symbol period. h is the modulation index, which takes the value of 0.5 in the GMSK modulation. $q(t)$ is the phase pulse of the modulator, which can be expressed as

$$q(t)=\int_{-\infty}^{t} g(\tau)\mathrm{d}\tau\ . \tag{3}$$

The frequency pulse $g(t)$ is limited to the interval $[0, L_0T_\mathrm{b}]$ and gives

$$g(t)=\frac{1}{2T_\mathrm{b}}\left\{Q\left[\frac{2\pi B}{\sqrt{\ln 2}}\left(t-\frac{L_0+1}{2}T_\mathrm{b}\right)\right]-Q\left[\frac{2\pi B}{\sqrt{\ln 2}}\left(t+\frac{L_0-1}{2}T_\mathrm{b}\right)\right]\right\}, \tag{4}$$

where L_0 is the length of the continuous symbols in Gaussian filter, and B is the 3 dB bandwidth. For BT_b is 0.3, L_0=3 is considered. $Q(t)$ is defined as

$$Q(t)=\frac{1}{\sqrt{2\pi}}\int_t^{\infty}\mathrm{e}^{-\tau^2/2}\mathrm{d}t\ . \tag{5}$$

The adversities in satellite detection include additive white Gaussian noise $n(t)$ and Doppler frequency offset f_d due to the satellite speed. The complex input of frequency estimation block in Fig.1 is

$$r(t)=\mathrm{e}^{\mathrm{j}(2\pi f_\mathrm{m}t+\theta)}+n(t)\ , \tag{6}$$

where $f_\mathrm{m}=f_0+f_\mathrm{d}$, f_0 denotes the intermediate frequency, and $\theta=\phi(t;\alpha)$ is the information bearing phase.

The GMSK signal is a series of single tone sine waves located symmetrically around the carrier frequency offset[15]. The knowledge of the training sequence and start flag of the AIS frame are available, and the re-modulated signal can be put in the form of

$$S(t)=\mathrm{e}^{\mathrm{j}\theta(t)}, \tag{7}$$

where

$$\theta(t)=\pi h\sum_i a_i q(t-iT_\mathrm{b}) \tag{8}$$

is the information bearing phase. The notations are the same as those in Eq.(2). Define a function as

$$x(t)=r_\mathrm{I}(t)S_\mathrm{I}(t)+r_\mathrm{Q}(t)S_\mathrm{Q}(t), \tag{9}$$

where $r_\mathrm{I}(t)$ and $r_\mathrm{Q}(t)$ denote the in-phase component and quadrate component of $r(t)$, respectively. Likewise, $S_\mathrm{I}(t)$ and $S_\mathrm{Q}(t)$ represent the in-phase component and quadrate component of $F(t)$, respectively

$$x(t)=\cos(\omega_0 t+\omega_\mathrm{d}t)+w(t)\ , \tag{10}$$

where $w(t)$ is the noise term with zero mean and variance of σ^2, and SNR is $1/(2\sigma^2)$. $x(nT_\mathrm{s})$ denotes the sample of $x(t)$ taken at $t=nT_\mathrm{s}$. Eq.(10) can be expressed as

$$x(nT_\mathrm{s})=\cos(\omega_\mathrm{m}nT_\mathrm{s})+w(nT_\mathrm{s}), 0\le n\le NL-1\ , \tag{11}$$

where $T_\mathrm{b}=NT_\mathrm{s}$. L is the length of the available data. Eq.(11) can be put in the form of

$$x(n)=\cos(\omega_\mathrm{m}n)+w(n), 0\le n\le NL-1\ . \tag{12}$$

Consider the DFT of $x(n)$, which is filtered by a window function. $X(\omega)$ is computed as[16]

$$X(\omega)=\frac{NL}{2}\frac{\sin\pi v}{\pi\prod_{n=-M}^{M}(v+n)}+z(\omega)\ , \tag{13}$$

where M is the order of the window function, and

$$v=\frac{T(\omega_\mathrm{m}-\omega)}{2\pi}, \tag{14}$$

where $T=LT_\mathrm{b}$ is the observation interval. Assuming that the noise term is negligible at moderately high SNR, the maximum spectral amplitude and its neighbor spectral amplitude can be denoted as

$$X_1 = \frac{NL}{2}\frac{\sin \pi u}{\pi \prod_{n=-M}^{M}(u+n)} \quad , \tag{15}$$

$$X_2 = \frac{NL}{2}\frac{\sin \pi (u-\alpha)}{\pi \prod_{n=-M}^{M}(u+n-\alpha)} , \tag{16}$$

where $u=[\omega_m T]/(2\pi)-l$ is limited to the interval $[-0.5,0.5]$, and l is the spectral number of X_1. Since $\alpha=\pm1$, Eq.(17) is then obtained as

$$\frac{X_1}{X_2} = -\frac{u-\alpha(M+1)}{u+\alpha M} \quad . \tag{17}$$

For the simplicity, makes M=0, and then the frequency offset f_d can be obtained as

$$f_d = \frac{1}{T}\left(l+\alpha\frac{X_2}{X_1+X_2}\right) - f_0 \quad . \tag{18}$$

When X_2 is the left neighbor spectral line of X_1, α is -1, otherwise, α is 1. As the noise term is considered, the variance of f_d is

$$Var\left[f_d\right] = Var\left[\frac{1}{T}\left(l+\alpha\frac{X_2}{X_1+X_2}\right) - f_0\right] = \frac{1}{L^2T_b^2}Var\left[\frac{X_2}{X_1+X_2}\right]. \tag{19}$$

The variance of f_d is related to $Var[X_2/(X_1+X_2)]$. For the time being, the calculation of Eq.(19) is equivalent to compute

$$Var\left[\frac{X_2}{X_1+X_2}\right] = Var\left[\frac{X_2/X_1}{1+X_2/X_1}\right], \tag{20}$$

where $X_1=P_1+Z_1$ and $X_2=P_2+Z_2$, P_1 and P_2 represent the maximum spectral amplitude and its neighbor spectral amplitude, and Z_1 and Z_2 denote the noise amplitudes corresponding to them, $Var[Z_1]=NL\sigma^2/2$. After some algebraic operations, we can get

$$\frac{X_2}{X_1} = \frac{P_2}{P_1}\frac{1+Z_2/P_2}{1+Z_1/P_1} . \tag{21}$$

For high *SNR* and large *NL*, Z_1/P_1=1 and Z_2/P_2=1. As a result, Eq.(21) can be expanded into infinite series form, and the high order term can be neglected. Eq.(21) takes the simple form as

$$\frac{X_2}{X_1} = \frac{P_2}{P_1}\left(1+\frac{Z_2}{P_2}-\frac{Z_1}{P_1}\right). \tag{22}$$

Substituting Eq.(22) into Eq.(20), we get

$$Var\left[\frac{X_2}{X_1+X_2}\right] = Var\left[\frac{1}{P_1+P_2}\frac{P_2+Z_2-\frac{P_2}{P_1}Z_1}{1+\frac{1}{P_1+P_2}\left(Z_2-\frac{P_2}{P_1}Z_1\right)}\right]. \tag{23}$$

Likewise, Eq.(23) can be expanded into infinite series form, and neglect the high order term, then produce

$$Var\left[\frac{X_2}{X_1+X_2}\right] = Var\left[\frac{P_2}{P_1+P_2}+\frac{P_1}{(P_1+P_2)^2}\left(Z_2-\frac{P_2}{P_1}Z_1\right)\right]. \tag{24}$$

For further simplification, Eq.(24) reduces to

$$Var\left[\frac{X_2}{X_1+X_2}\right] = \frac{P_1^2+P_2^2}{(P_1+P_2)^4}\frac{NL}{4SNR} . \tag{25}$$

Considering M=0, substituting Eq.(15) and Eq.(16) into Eq.(25), then

$$Var\left[\frac{X_2}{X_1+X_2}\right] = \frac{\pi^2}{NL \times SNR}\frac{u^2(\alpha-u)^4+u^4(\alpha-u)^2}{\sin^2 \pi u} . \tag{26}$$

It is readily seen that Eq.(26) is minimum when u=0.5, thus the minimum variance of f_d is

$$Var\left[f_d\right] = MCRB(f_d) = \frac{\pi^2}{32NL^3T_b^2}\frac{1}{SNR} . \tag{27}$$

As in the analysis, Eq.(27) is the minimum variance of f_d, so the MCRB is lower than the true CRB.

The following section will give the simulation results of the performance of the estimator described in this paper. The performances are described in normalized frequency estimation mean square error (*MSE*), which is defined as

$$MSE = \frac{1}{D}\sum_{i=1}^{D}\left[(\hat{f}_d - f_d)T_b\right]^2 , \tag{28}$$

where D is the number of Monte Carlo simulations. With GMSK modulation, the length of the continuous symbols in Gaussian filter L_0 and the 3 dB bandwidth T_bB are 3 and 0.3 respectively. The training sequence and start flag in AIS frame are available for data aided, totally 32 bit. The oversampling factor N is set to 8. The symbol duration T_b is 1/9 600 s.

Fig.2 shows performance comparison between the proposed estimator and those in the literature. For the sake of simplicity, let A be the proposed estimator in this paper, B and C denote the estimators in Ref.[7] and Ref.[6], respectively, and the MCRB in Eq.(27) is used as a benchmark. The estimators in Ref.[7] and Ref.[6] were operated in the baseband, i.e. the intermediate frequency was 0 Hz. To be consistency, the intermediate frequency of the proposed estimator in this simulation was set as 0 Hz. As seen from Fig.2, B has poor performance, and C has higher estimation accuracy than B. A has much better performance than C, especially when *SNR* is less than 3 dB. Additionally, its *MSE* is about 1.7 dB above the MCRB when the *SNR* is higher than 3 dB.

Fig.3 illustrates the *MSE* versus normalized frequency offset f_dT_b when *SNR* is 20 dB. In the following simulations, the intermediate frequency is 24 000 Hz. The estimation range of algorithm A is coarsely more than the symbol rate and is larger than that of the other algorithms. Also, it covers the frequency offset range of the satellite-based AIS.

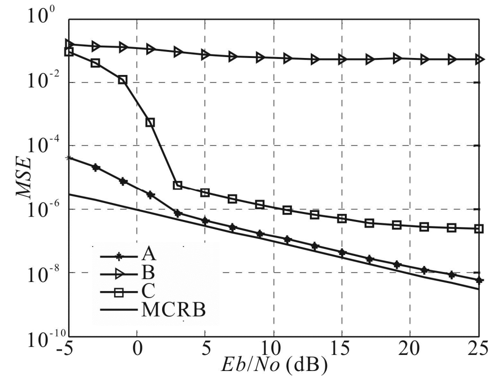

Fig.2 Performance comparison of different frequency estimators for GMSK

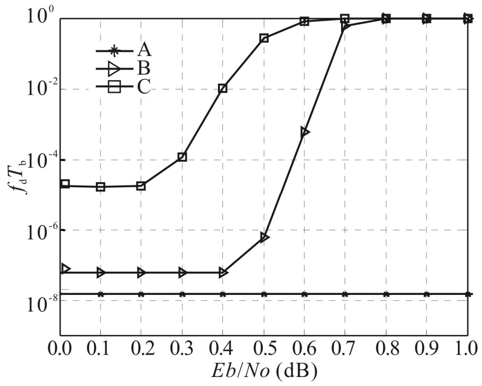

Fig.3 Effect of frequency offset on performance of different frequency estimators

In the satellite-based AIS communication system, large Doppler frequency offset occurs in the received signals, as well as the time delay. Thus, the estimator should be anti-time delay more or less. As Viterbi algorithm (VA) is adopted in the demodulator, simulation shows that the *BER* meets the need of the satellite-based AIS when frequency offset *MSE* is lower than 10^{-4}. Fig.4 shows the *MSE* of the proposed estimator versus *SNR* for different timing errors. It is clearly demonstrated that the performance deteriorates further with the time delay increasing. The *MSE* is lower than 10^{-4} when timing error is a half of the symbol period, which still covers the tolerance of VA.

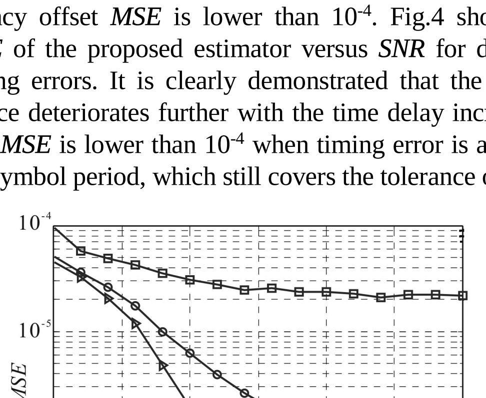

Fig.4 Effect of time delay on performance of the proposed estimator

Subjecting to the signal separation performance, the input signal for frequency estimation is not pure, and some extremely weak interference signals are contained. Fig.5 shows the effect of *SIR* on the performance of the proposed estimator, in which the frequency offset is 4 000 Hz. It shows that the *MSE* is increasing with the *SIR* increasing at the same *SNR*. Resulting from the low *SNR*, the effect of *SIR* on the estimation performance is very small, and it becomes visible when *SNR* is above 5 dB. As mentioned before, the performance is accredited for the satellite-based AIS even when *SIR* is 3 dB.

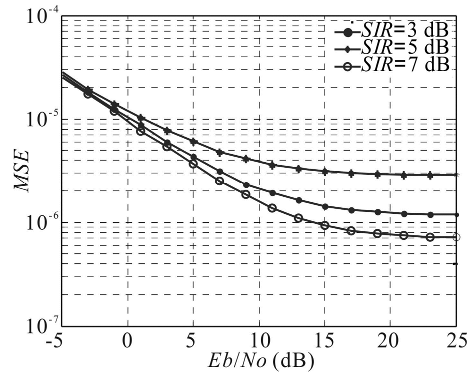

Fig.5 Effect of *SIR* on performance of the proposed estimator

In Fig.6, the performance of the estimator is plotted with different available data lengths. The longer pilot data length results in much better estimation performance. In Fig.1, the output data of the demodulator is 256 bit, which is available for message re-modulation to counteract the interference signal. Obviously, the estimator has good performance when the available data length is 128 or 224.

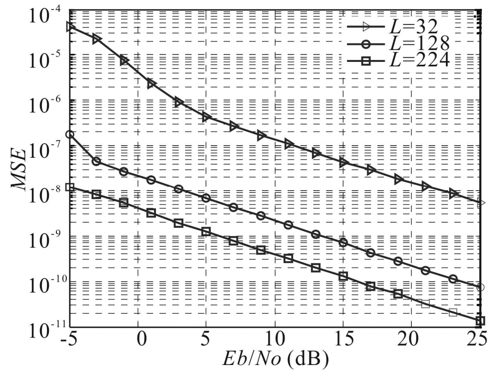

Fig.6 Performance of the proposed estimator with different available data lengths

An accurate frequency offset estimator for the satellite-based AIS is proposed in this paper. The estimator can operate in intermediate frequency. The performance of the frequency estimator and that corresponding to a timing error, as well as the *SIR* and the available data length have been plotted. The estimator has better performance than those in the literature. Additionally, the variance of the estimator is calculated, and the performance of the estimator is about 1.7 dB above the MCRB. The estimator has very low complexity and is easy to implement, which is very suitable for the satellite-based AIS.

References

[1] Boundy N., LeMaitre J. and Millerioux J. P., Results of Measurement Campaign for Characterization of AIS Transmitter, Advanced Satellite Multimedia Systems Conference and 12th Signal Processing for Space Communication Workshop, Baiona, 258 (2012).

[2] Anindya H., Binay K.S. and Kalyan K.B., Beam Scanning for Reception Performance Improvement of Satellite-based AIS, 2015 IEEE International Conference on Aerospace Electronics and Remote Sensing Technology (ICARES), Bali, 1 (2015).

[3] Panyuan X, Taosheng Z, Lianghui D, Feng Y, Liang Q and Hongxing L, Practical Concern Analysis on the Detection Probability for Satellite-based AIS, The 22nd Asia-Pacific Conference on Communications (APCC2016), Yogyakarta, 388 (2016).

[4] Sriram J, Jyothendar P, Aditya V. G and Manoj K. M, Satellite-based AIS Receiver for Dense Maritime Zones, 2017 9th International Conference on Communication Systems and Networks (COMSNETS), Bangalore, 15 (2017).

[5] Burzigotti P., Ginesi A. and Colavolpe G., Advanced Receiver Design for Satellite-based AIS Signal Detection, 5th Advanced Satellite Multimedia Systems Conference and 11th Signal Processing for Space Communications Workshop, Cagliari, 1 (2010).

[6] Hua P., Jing L. and Lingdong G., Non-data-aided Carrier Frequency Offset Estimation of GMSK Signals in Burst Transmissions, 2003 IEEE International Conference on Acoustics, Speech, and Signal Processing, Hong Kong, 576 (2003).

[7] Kay S. M., IEEE Transactions on Acoustics, Speech and Signal Processing **37**, 1987 (1989).

[8] Fitz M. P., Planar Filtered Techniques for Burst Mode Carrier Synchronization, Global Telecommunications Conference, Phoenix, 365 (1991).

[9] Luise M. and Reggiannini R., IEEE Transactions on Communications **43**, 1169 (1995).

[10] Tuanfeng W., New Data-aided Frequency Estimation Algorithm based on Discriminator for GMSK Signals, Neural Networks and Signal Processing, 2003 Proceedings of the 2003 International Conference on, Nanjing, 1706 (2003).

[11] Sam R and Elias A, IEEE Communications Letters **7**, 549 (2003).

[12] Souden M., Affes S., Benesty J. and Bahroun R., IEEE Transactions on Signal Processing **57**, 4148 (2009).

[13] Linqian L, Yiqiao F, Wenbo Z and Nan C, Extended Kalman Filter for Carrier Frequency Offset and Carrier Phase Noise, 2017 Conference on Lasers and Electro-Optics (CLEO), San Jose, 1 (2017).

[14] Shexiang M., Xiaojuan Liu and Xin M., Data-aided Parameters Estimation of Satellite-based AIS Signals, International Conference on Electronics and Information Engineering (ICEIE), 862 (2013).

[15] Guoqing Q. and Xinle J., Acta Electronica Sinica **29**, 1164 (2001).

[16] Kay S. M., Modern Spectral Estimation, Prentice-Hall Signal Processing Series, Oppenheim, Prentice-Hall, Englewood Cliffs, New Jersey (1988).